Optional Additional Information

PROGRESS REPORT NO. 6

Annual Report for the Period 6/15/02--6/14/03

Managing Tight Binding Receptors for New Separations Technologies

EMSP Project Number 73831

Grant Number: DE-FG07-96ER14708

Recipient: Research Support & Grants Administration
University of Kansas
2385 Irving Hill Road, Youngberg Hall
Lawrence, KS 66044-7553

Recipient Project Director: Daryle H. Busch
Chemistry Department
University of Kansas
Lawrence, KS 66045
785-864-5172

Co-Investigator: Richard S. Givens
Chemistry Department
University of Kansas
Lawrence, KS 66045
785-864-3846

Toward a Soil Poultice for the Remediation of Metal Ion Contamination

An Imprinting System based on Hydrogen Bonding. In our first explorations we chose to use a tetradentate macrocyclic ligand, N,N',N'',N'''-tetra(2- carbamoylethyl)-1,4,8,11-tetraazacyclotetradecane (4cyclam), to provide strong metal ion binding, with four appended arms that terminate in amide functions to provide hydrogen bonding with corresponding groups in the polymer (Structure 1). Nickel(II) ion was chosen for these studies because of the kinetic inertness of the square planar complexes it forms with tetraazamacrocycles. Because covalent interactions tend to involve slow kinetics we use those that are non-covalent for the affinity between the MIP and the imprinting metal complex. The immediate issue is "can non-covalent interactions be strong enough to produce the proposed new methodology?" The literature indicates that imprinting using, for example, hydrogen bonding supports only 10 to 15%, certainly less than 20%, re-binding capacity. An equally compelling issue is the relationship of the combined advantages of selective complex formation and selective binding of the complex to the polymer. Further, are these macroporous polymers durable enough to be used in a separations

methodology? In considering these issues, binding and selectivity have been studied at both the complex formation and the polymer/imprint level.

Metal Ion Selectivity of the Test Ligand. As reported previously, when the complexing ability and metal ion selectivity of the macrocyclic ligand (A4cyclam, **Structure 1**) were

Structure 1

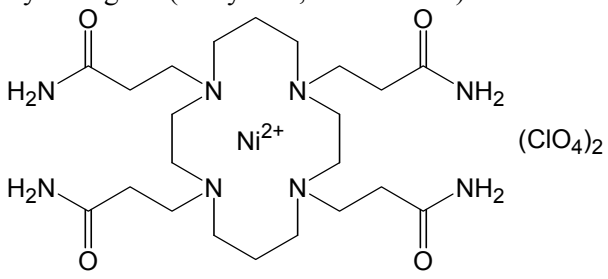

investigated by equilibrium methods, it was Found that Cu(II)and Hg(II) bind billions of times more strongly that other common metal ions, suggesting a possible application for the prototypic soil poultice.

Optimizing Hydrogen Bonding in MIPs. Table 1 summarizes the synthetic parameters, surface characterization, and rebinding capacity of a number of photochemically (indicated by "P") and thermally (indicated by "T") initiated MIPs, as well as a number of "control polymers" (no imprint). The morphological data show that all polymer samples are macroporous (surface in the defining range, 50-1000 m^2/g).[35] For both modes of polymer initiation, surface area and pore volume decreased with the incorporation of the imprint molecule.

Table 1. Characterization and Nickel Rebinding Capacity of Macroporous Polymers

Polymer[a]	T/(˚C)/Solvent/ Initiator[b]	Surface area (m^2/g)	Pore volume (cm^3/g)	% Ni re-uptake[d]
P1 (Blank)	4/MeCN/AIBN	271	0.56	11.7
P2	4/MeCN/AIBN	229	0.51	13.6
P3	4/MeCN&MeOH/AIBN	162	0.25	8.7
P4 (Blank)	4/MeCN&MeOH/AIBN	----	----	18.4
P4	4/MeCN&MeOH/BEE	63	0.15	8.4
T1 (Blank)	50/MeCN&MeOH/AIBN	365	0.51	16.8
T2	50/MeCN&MeOH/AIBN	311	0.38	26.8
T3	40/MeCN&MeOH/ABDV	335	0.43	16.9
T4 (Blank)	40/MeCN&MeOH/ABDV	----	----	13.6
T5	30/MeCN&MeOH/ABDV	305	0.34	19.5
T5[c]	30/MeCN&MeOH/ABDV	278	0.33	24.3
T6 (Blank)	30/MeCN&MeOH/ABDV	----	----	19.3

[a] P: photochemically initiated polymer; T: Thermally initiated polymer. [b] MeCN/MeOH=1, [c] Treated at 120 ˚C overnight before rebinding experiment. [d] Based on the starting nickel complex or acrylamide.

Since relatively weak non-covalent interactions are favored by low temperature,[1,2] our first polymers were formed by photoinitiation at 4ºC, but all rebound less than 15% of the theoretical capacity and showed very little increase in rebinding capacity attributable to imprinting (MIP P2 bound only 1.16 times the non-imprinted P1). The inferior performance of photo-polymers has been attributed to the heterogeneous polymerization process[3]. In contrast, thermally initiated polymers displayed larger surface area[4] and much higher rebinding. In fact, the observed value of 26.8% is superior to those previously reported for polymers imprinted by hydrogen bonding alone.[1,5] Simultaneously, rebinding capacity attributable to the imprinting effect was greater (T2 and T1, 26.8/16.8= 1.60).

According to the work of Shea *et al.* on the chromatographic separation of enantiomers, the performance of MIPs was improved upon heat treatment after removal of the imprint.[5] Accordingly, T5 was heated at 120ºC overnight before rebinding and the re-uptake increased from 19.5% to 24.3%. Also, T2 was used repeatedly and reuptake increased from 26.8% to 35.0% in the 4th run. Very recently Nicholls *et al.* reported[6] that polymers retained their affinity (≥95%) for the imprint on exposure (24 h) to 10 M HCl. In our work T2 was shown to be resistant even to the very strong oxidizing agent, concentrated nitric acid, although the surface area and pore volume were decreased from 311 m^2/g and 0.38 cm^3/g to 229 m^2/g and 0.28 cm^3/g, respectively.

The use of *N*,*N*′-ethylenebisacrylamide (EBA) as crosslinking monomer**.** Polymer recognition of the metal complex was also found with the functional groups located on the crosslinker, *N*,*N*′-ethylenebisacrylamide (EBA), in the absence of acrylamide. Remarkably, the nickel reuptake corresponded to 187.7% of the amount of imprint originally used. This excess capacity reflects the large excess of amide groups on the crosslinker. On the other hand, the value for the control polymer **P7** was only 108.7% (calculated on the basis of the imprint in **P8**). The difference 79%, indicates a high rebinding percentage at the imprinted sites. The corresponding copper complex, $[Cu(A4cyclam)](ClO_4)_2$, was used in parallel experiments with essentially the same results. It must be emphasized that this remarkable imprinting capacity is due to hydrogen bonding alone.

Table 2. Nickel re-uptake of EBA polymers

Polymer [a]	Ni used in the polymerization (mol Ni/mol EBA)/ (mg Ni/g EBA)	Ni re-uptake (mg Ni/g EBA)	% Ni re-uptake [c]
P7 (blank)	0	20.13	------
P8	(1/19)/18.51	34.74	187.6
P9	(1/9)/38.03	30.00	78.9
P10 [b]	(1/2)/165.9	27.11	16.3

[a] Polymerization conditions: initiated by AIBN at 50ºC; acetonitrile/methanol=1/2 for **P7**-**P9**, 1/1 for **P10**; [b] Treated with HNO_3 after soxhlet extraction; [c] Based on the starting nickel complex.

Introduction of a Second Mode of Interaction, Electrostatic Attraction. The vinylsulfonate salt of the nickel(II) complex with the A4cyclam, (*N, N', N'', N'''*-tetra(2-carbamoylethyl)-1,4,8,11-tetraazacyclotetradecane)nickel(II) vinylsulfonate, $[Ni(A4cyclam)](CH_2{=}CHSO_3)_2$, was synthesized and used in the molecularly imprinted polymer investigation. This imprint differs

from the previous one in that the counter ion of the imprinting salt acts as a functional monomer and becomes incorporated into the polymer. This adds electrostatic attraction to the hydrogen bonding. Of course, polymers imprinted with Ni(A4cyclam)]$(CH_2=CHSO_3)_2$ are ion exchange materials, not analogous to chromatographic supports. The new polymer was first treated by soxhlet extraction, and then further treated either with concentrated nitric acid or with methanolic ammonium chloride to remove the imprint. As expected, a much higher nickel ([Ni(A4cyclam)]$(ClO_4)_2$) re-uptake was observed; 44.8% for the sample treated with nitric acid and 60.0% for the sample treated with ammonium chloride. The difference suggests that nitric acid damages the binding sites. Further, the imprinting effect is far more evident when compared to the blank polymer (60.0/16.8=3.57). Thus rebinding capacity increased by a factor of between 3 and 4.

The minor ligand, vinyl pyridine as a second (or third) mode of interaction**.** When vinyl pyridine was added as a second functional monomer (in addition to acrylamide) rebinding was increased by a factor of about three. Incrementally increasing the concentration of 4-vinylpyridine by replacing equivalent amounts of acrylamide affords substantial improvement in the imprinting effect for the MIP's (Q4, Q5, Q6 through Q7). Like electrostatic attraction, this mode of interaction offers promise of synergistic bimodal binding of the rebound imprint.

Table 3. Rebinding capacities for polymers of various 4-vinyl pyridine/acrylamide ratios for the imprint [Ni(A4cyclam)]$(CIO4)_2$

	Molar ratios - % (Vpy/Acrylamide)	Ni levels-ppm (rebound;residual)	Percent Ni Uptake
Q9	(0 / 100)	(1.55; 0.29)	18.1%
Q10 (Blank)	(0 / 100)	(1.15; 0.03)	(16.1)
Q4	(33 / 67)	(2.12; 0.19)	28.2%
Q6	(50 / 50)	(2.36;0.21)	31.2%
Q5	(67 / 33)	(3.34;0.18)	46.9%
Q7	(100 / 0)	(3.68/0.19)	52.2%
Q7 (Blank)	(100 / 0)	(2.71;0.19)	37.7%

The data in Table 4 show a striking effect of excess functional polymer. As the excess of the functional monomer (4-vinylpyridine) increases from 2:1 to 6:1, the rebinding capacity increases from barely detectable to 95%.

Table 4. Effect of varying the monomer-to-imprint mole ratio on rebinding performance for 4-vinyl pyridine MIP's templated against A4cyclam)Ni(II) perchlorate

Polymer[a]	Imprint :monomer mole ratio	Crosslinking value (%)	Rebound polymer for HNO_3 digestion (g)	Ni levels (ppm) in a 50mL extract (rebound;residual)	Rebinding value (%)
P30	1:1	97.3	0.0265	0.976; 0.387	8
P31	1:2	94.7	0.023	1.37; 0.315	17.0
P31(Blank)	1:2	94.7	0.0267	1.19; 0.05	15
P32	1:3	92.2	0.0257	2.74; 0.238	37.0
P33 [a] P7 [a]	1:4 1:4	89.9 89.9	0.0265 0.0265	3.41; 0.47 3.68; 0.19	43.2 52.2
P34	1:6	85.6	0.0265	6.48: 0.25	95.5
P34(Blank)	1:6	85.6	0.0228	2.0; 0.01	35.6

[a] Independent batch preparations under identical conditions

Both the minor ligand binding (4-vinylpyridine) and hydrogen bonding give striking results as the excess of polymer binding sites increases. This is shown most clearly by comparing each parameter with a value from a blank experiment as shown in Table 5. Here the performance of the imprint improves by 2.7 times as much as the blank, for 4-vinylpyridine, and 3.5 times for acrylamide.

Table 5. Rebinding affinities of 4-vinylpyridine and acrylamide MIP's for Ni(A4cyclam)]$(ClO_4)_2$ versus their respective controls to probe selectivity indications at varied monomer content levels

Binding monomer	Imprint /monomer ratio	Identity, type	Cross linking (%)	Polymer wt (g) for HNO_3 digestion	Ni (ppm). (rebound residual) (50 mL)	Capacity (%)	Affinity ratio (a) / (b)
4-vinyl-pyridine	1:6	P34 (a)	85.6	0.0265	6.48; 0.25	95.6	2.7
		P34 Blank	85.6	0.0228	2.0;0.01	35.6	
	1:2	P31	97.3	0.0230	1.37;0.315	17	1.2
		P31 Blank	97.3	0.0257	1.19; 0.21	14	
Acrylamide	1:12	P53	82.3	0.0265	5.01; 0.36	74.4	3.5
		P53 Blank	82.3	0.0255	1.3; <0.01	21.2	
	1:4	P9	93.3	0.0265	1.55; 0.29	18.1	1.1
		P10 Blank	93.3	0.0258	1.15; 0.03	16.1	

(a) = Imprinted (b) = Control

Copper(II) imprinting and rebinding gave parallel behavior but with lower binding. Replacing 4-vinylpyridine with 2-vinylpyridine, in the absence of a hydrogen bonding monomer, produced an "imprinted" polymer with essentially zero binding capacity. The cumulative results have made it clear that informed design of MIPs may produce extremely good non-covalent rebinding behavior, at least in the media investigated to this point.

Designing Experiments to Determine Selectivity. Recall that two metal ions, copper(II) and mercury(II), show greater affinities for the ligand A4cyclam than the several other metal ions studied. The affinity of A4cyclam for copper(II) exceeds that for nickel(II) by some 12 orders of magnitude. A single experiment has been performed in an attempt to observe the combination of the two selective processes (complexation and rebinding). One molar equivalent each of nickel(II) perchlorate, copper(II) perchlorate, and A4cyclam were combined in a methanol solution and the previously extracted, metal ion free, [Cu(A4cyclam)]$(ClO_4)_2$ imprinted polymer **P14** was treated with this solution. ICP analyses revealed a substantial 12 to 1selectivity in favor of copper.

Studies on Switch-binding with Generation 1 Ligands

In the switch-binding concept, a linear ligand (L^4 in Scheme 1 below) binds very rapidly to the targeted metal ion, Ni^{2+}. This linking is followed by ring closure about the metal ion to form a complex of the macrocyclic ligand (L^8). In theory, the ring closure could be very rapid, in which case, switch-binding will have occurred more rapidly than the same metal ion (Ni^{2+}in this case) could have bound to the free macrocycle (assuming it would be available).

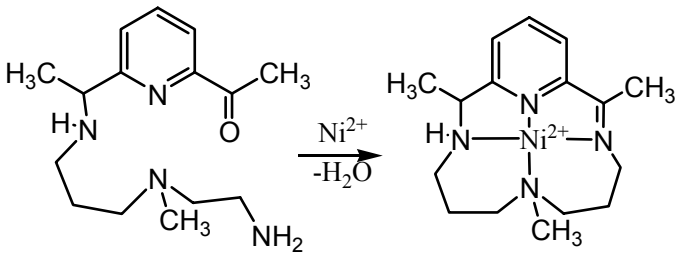

L^4 $Ni(L^8)^{2+}$

Scheme 1

Early studies in this work on the switch-binding concept centered on the development of a synthetic methodology adequate to provide a reliable supply of Generation 1 switch-binding ligands (L^4). The first few grams of L^4 were used (1) in batch experiments to demonstrate unequivocally that when L^4 combines with nickel(II) ion the desired macrocyclic complex is indeed formed. (2) First samples of L^4 also made possible a very limited number of kinetic measurements and these have been reported previously and were viewed as supporting the concept.[7] Although the synthetic procedures for L^4 and L^8 have changed only in detail, much of our researchers' time continues to be spent in making the ligands necessary for this work.

The reaction of Ni^{2+} with L^4 involves reactions in two time regimes, the first in fractions of seconds and the second in hours. Both processes are accompanied by increases in visible light absorbance, as expected for formation of a square planar nickel(II) complex. In the discussion to follow, capital K represents equilibrium constants and lower case k, rate constants. The equilibrium constants for L^4 were determined in our earlier studies. Using our Hi Tech stopped flow spectrophotometer, measurements for the fast process were made as functions of pH (pH range 5.6 to 7) and [L^4] (10 to 30mM, held in excess; I = 0.2 KNO_3, 25 ^oC) in the presence of nickel(II), whose spectral absorbance at 380 nm was the reaction variable. Study of the dependence on [L^4] revealed the expected behavior in which a forward reaction rate (formation of the complex) is proportional to [L^4], and a reverse reaction rate is independent of [L^4]. The pH dependence reflects the fact that the ligand exists in solution as a mixture of species differing in the extent of protonation. The mechanism is described by the following equations:

$$Ni^{2+} + HL^{+} \leftrightarrow NiHL^{3+} \; ; \qquad k_{HL} = 17.3\ (\pm 0.5)\ M^{-1}s^{-1}$$

$$H_2L^{2+} \leftrightarrow HL^{+} + H^{+} \; ; \qquad K_{D2} = 5.9x10^{-8}\ M$$

$$Ni^{2+} + H_2L^{2+} \leftrightarrow NiH_2L^{4+} \; ; \qquad k_{H2L} = 2.49\ (\pm 0.03)\ M^{-1}s^{-1}$$

The fast process proceeds with a half-life in the 40 millisecond range, and the first events involve the usual reversible binding of one or two ligand sites to the metal ion.

The slow reaction presents a greater challenge. Very commonly macrocyclic ligands first form complexes in conformations that do not produce the most stable final product. Consequently, slow reactions often follow macrocyclic complex formation. The question then becomes "is our slow reaction such a rearrangement or is it the ring closure step?" Because the ligand is rare and needs to be used in excess, the slow reaction was studied over the limited pH range from 6.9 to 7.9, with a constant [Ni^{2+}] = $1.0x10^{-4}$M in a 12 to 70 fold excess of L^4 over Ni^{2+} (I = 0.2M., 25^oC). The kinetics are nicely pseudo first order and the rate is insensitive to [L^4]. A non-linear increase in rate with pH was observed. The model that quantitatively describes the slow reaction involves a rapid proton dissociation followed by a rate-determining rearrangement step.

$$NiLH^{3+} \leftrightarrow \{NiL^{2+}\}_{intermediate} + H^{+}; \quad \text{fast, } K_{MHL} = 1.1\times10^{-7}\,M$$

$$\{NiL^{2+}\}_{intermediate} \longleftrightarrow NiL^{2+}; \quad \text{slow, } k_{ML} = (4.2 \pm 0.2)\times10^{-5}\,s^{-1}$$

At room temperature this slow reaction proceeds with a half-life of 5 hours around neutral pH. The reaction is solely due to the monoprotonated precursor complex, $NiLH^{3+}$. Further, because the equilibrium constant for the deprotonation step has been found to be about 10^{-7} M, a substantial amount of NiL^{2+} is available for reaction.

Since the rapid and slow processes are so well separated in time, mass spectrometric studies were conducted to demonstrate the compositions of the intermediates and products. Scheme 1 shows that the ligand loses a mole of water when macrocyclization occurs. During the short reaction times (milliseconds to minutes) the nickel-containing intermediates were shown to contain only the beginning ligand, L^4 (the mole of water is still in the ligand composition). On the time scale of hours, the mass spectrometry clearly establishes the appearance and eventual dominance of the macrocyclic complex. Therefore for this system, macrocyclization is slow compared to initial complex formation.

Studies on Switch-binding with a Generation 2 Ligand

Generation 2 ligands for switch-binding take advantage of a macrocycle as a basic structural element for capturing ions. Attached to the macrocycle is a lariat arm capable of additional interactions in the presence of targeted ions, including conversion of the ligand to a molecular cage within which the templating metal ion is captured, as illustrated in Scheme 2. This derivative offers a faster alternative to the capture of metal cations because the cation can avoid the high-energy transition state that requires it to squeeze between the bridge arms of the cryptand in order to reach the central cavity.

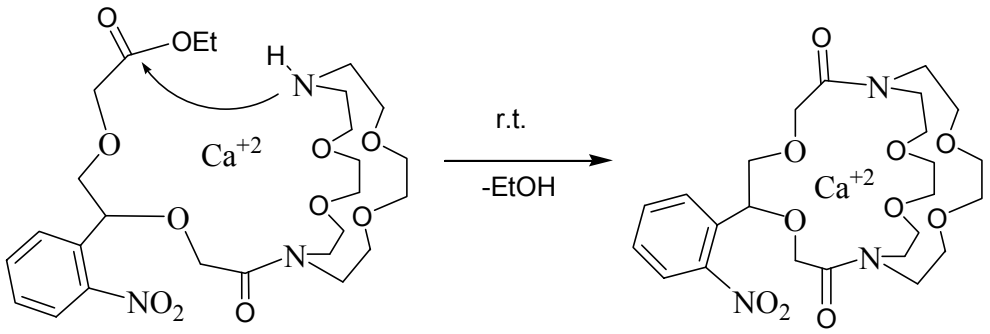

Scheme 2

The synthetic sequence and the current stage of that synthesis are indicated for Lariat ether in Scheme 3. Steps 1 – 4 have been accomplished and steps 5 - 9 will be completed during the next month.

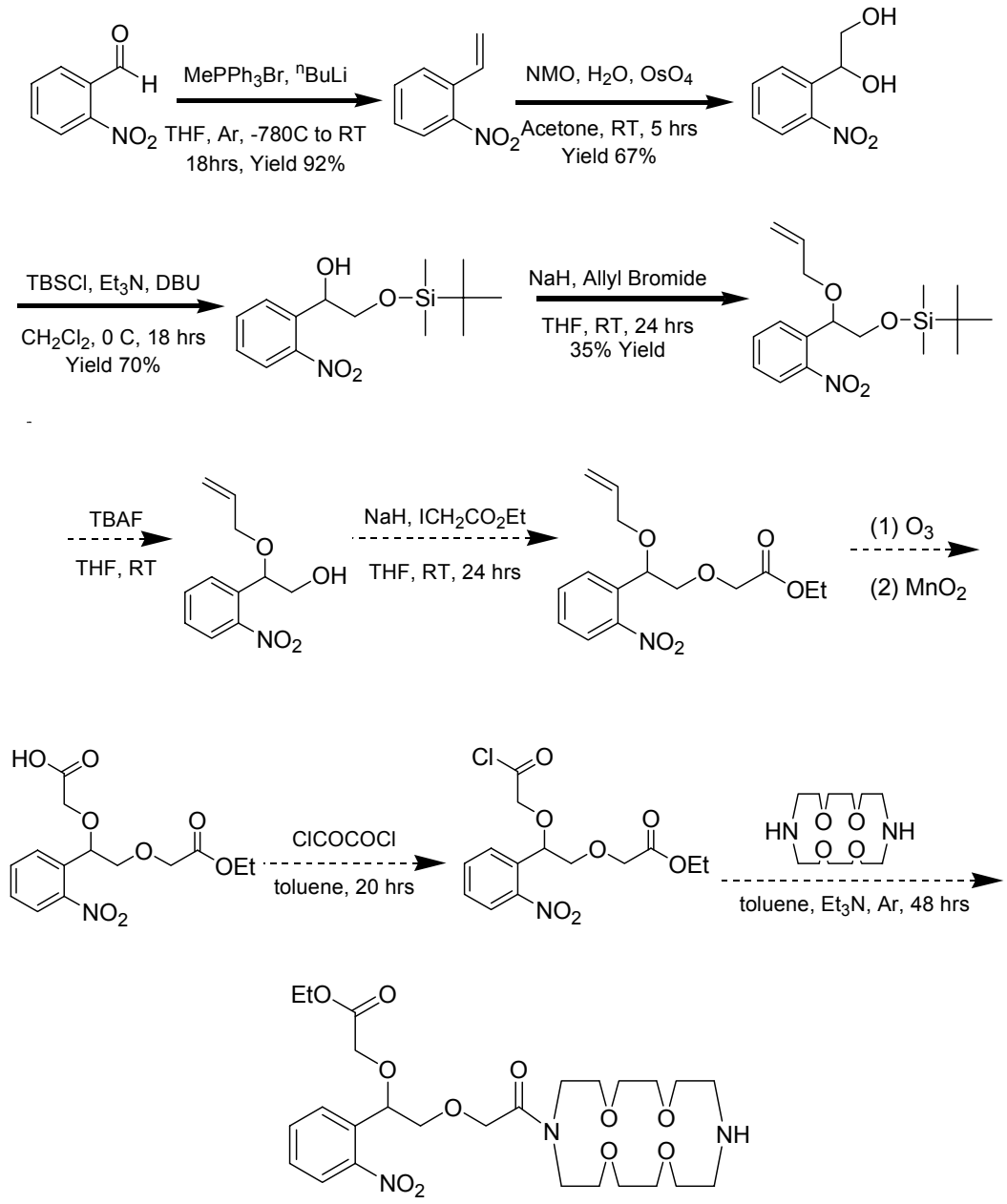

Scheme 3. Synthetic Route to Lariat Macrocycle

Studies of the Switch-release Principle

Selective capture followed by isolation and then photochemically initiated release of specific ions has been the goal of our research program. Our approach involves first the selective encapsulation of a metal ion by a photoreactive cryptand crafted to capture ions based on size and coordination. We chose the o-nitrobenzyl group for photoactivation based on our extensive review of the photochemical literature.[8,9] Our choice for a target is the photoactive *o*-nitrophenyl cryptand (oNPC)[10] that we have synthesized in six steps from readily available *o*-

nitrobenzaldehyde in an overall yield of 22%. The synthetic strategy of cryptand synthesis involves: 1) a stepwise build-up of a photocleavable triethylene glycol ether bridge with an *o*-nitrobenzyl group in the center and terminated at each end by acid chloride functions and 2) condensation of the bridge with the macrocycle, 1,4,10,13-tetraoxa-7,16-diazacyclooctadecane, giving the photoactive cryptand. The yields have been significantly improved resulting in larger quantities of material available for testing.

The capture of selected ions has been demonstrated with Ca^{+2}, Co^{+2}, Mn^{+2}, K^{+}, and Na^{+}. For example, the Ca^{+2} cryptates were synthesized by stirring the cryptand with excess $Ca(BF_4)_2$ or $Ca(SCN)_2$ in methanol followed by filtration and concentration. We have characterized these cryptates by mass spectrometry and NMR where possible. We are in the process of attempting crystallization for x-ray structure determinations of selected members of the series. These ionic cryptates are generally water-soluble and are easily maneuvered for chemical and photochemical studies. We have selected two for initial photochemical investigation, the Ca^{+2}-cryptate and the Co^{+2}-cryptate, to test the effect of spin multiplicity of the ion on the photochemistry. Diamagnetic groups should have no effect but paramagnetic ions could potentially quench the photochemistry by deactivation of the excited state if the triplet manifold were the reactive state of the chromophore.

Photochemistry of Cryptand. An aqueous solution of the photolabile cryptand (10^{-3}M) was photolyzed at 300 nm and the photoproducts analyzed by the ^{1}H-NMR, IR and UV-visible spectroscopy. The ^{1}H NMR shows a steady decrease of the absorptions of the four diastereomeric benzylic proton signals between 5.0-5.5 ppm and the appearance of new peaks at 4.77, 4.2, and 4.1 ppm during the irradiation. The new peaks were assigned to three methylene peaks of the opened macrocycle, clearly indicating ring opening of the cryptate. Likewise, the IR spectrum recorded after photolysis shows a new carbonyl and hydroxyl absorptions at 1711 cm^{-1} and 3407 cm^{-1}, respectively. UV-visible studies show a decrease in intensity of the peak at 265 nm and the appearance of new peak at 310 nm, further supporting the open macrocyclic structure. (Scheme 4; Figure 1).

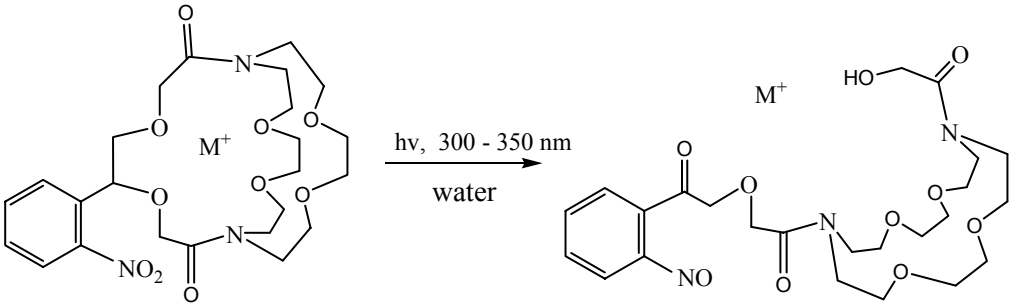

1
1a, $M^{+} = Ca^{+2}$

2

Scheme 4. Photoinduced ring opening of Cryptand 1 and Ca^{+2} Cryptate 1a

^{1}H NMR studies of calcium cryptate(**1a**). The $Ca(BF_4)_2$ cryptate (115 mg; 14.3 mM) was dissolved in 5 mL of D_2O along with 10 μL of acetonitrile as an internal standard for the ^{1}H NMR measurements. The UV absorption at 265 nm (ε = 3900 M^{-1} cm^{-1}) was measured. A 1 mM

D_2O solution of the Ca^{2+} cryptate was photolyzed at 300 - 350 nm and the disappearance of the benzylic peaks at 5.2 ppm (^1H NMR) and the change in the UV-vis spectrum (Figure 1) were used to measure the rate of disappearance of the cryptate. The relative rates of photochemical ring opening were not dependent on the presence of calcium.

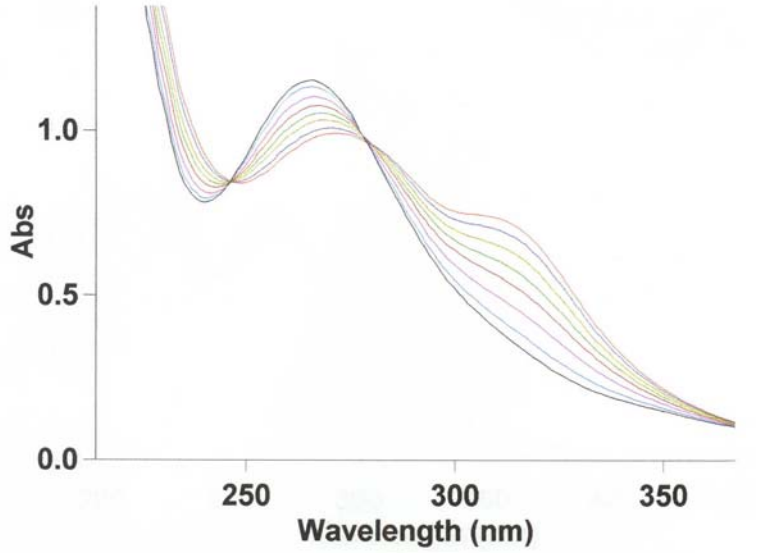

Figure 1. UV-visible absorption spectra of $Ca(BF_4)_2$ cryptate **1a** in water (10^{-4} M) during photolysis for 10 min with 1 min intervals at 300 nm (Rayonet Photoreactor).

Quantum efficiencies of Ca^{+2} Cryptate disappearance. The quantum efficiency of $Ca(BF_4)_2$ cryptate disappearance was determined in water at 300 nm using the potassium ferryoxalate actinometry. Similarly the quantum yield of disappearence of the $Ca(SCN)_2$ cryptate was determined to be 0.44 (Figure 2).

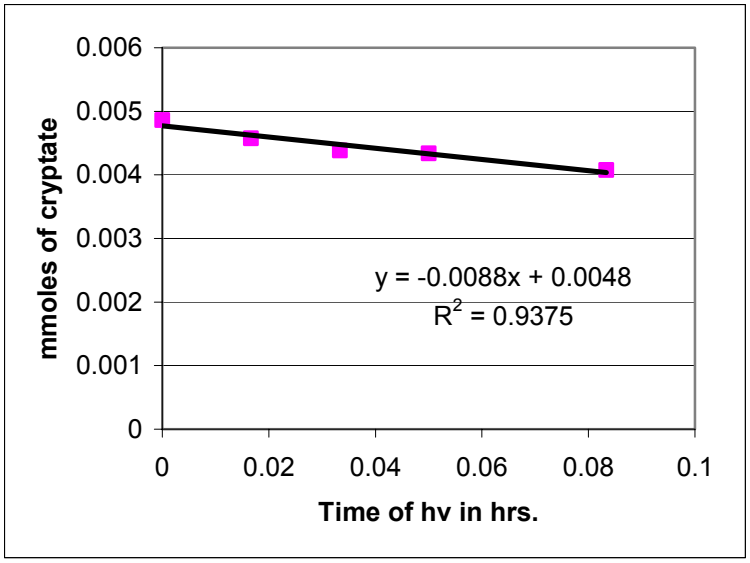

Figure 2: Quantum efficiency for the disappearance of $Ca(SCN)_2$ cryptate.

Quantitative analysis of the Ca^{+2} release using Calcium electrode. The release of calcium was quantified using a calcium electrode. A 2 mL solution of $Ca(BF_4)_2$ cryptate (13.8 mM; 1 eq $Ca(BF_4)_2$) in water was added to 17.6 mL of MOPS buffer solution (pH 7) containing 0.4 mL of 4M KCl (to adjust the ionic strength). A 3mL aliquot of the cryptate solution was taken each time into a cuvette and photolyzed at 300nm (Rayonet Reactor) for 0, 1, 2, 4, and 6 min and the calcium electrode signal recorded. The results show that when one equivalent of $Ca(BF_4)_2$ is stirred in the presence of the cryptand, 95% of the Ca^{+2} was incorporated into the cryptand. It was found that upon photolysis of the resulting cryptate in water, ~ 40% of the Ca^{+2} was released, based on the disappearance of the cryptate. The quantum efficiencies of the Ca^{+2} uptake, photorelease from the cryptate, and affinity for the opened cryptate (macrocycle) were determined. The results for the release are shown in Table 6.

Table 6: Photochemical release of calcium from its cryptate[a]

Time of hν @ 300nm	mV	Ca^{+2} released in mmoles	% of Ca^{+2} released based on cryptate concentration	% of Ca^{+2} released based on open cryptate concentration
0	-8	0.000088	0	0
1	-7	0.000098	0.7	14.70
2	-5	0.000120	2.4	22.53
4	-3	0.000147	4.5	27.60
6	-2	0.000163	5.8	37.47

[a]A 1.38 mM cryptate buffer solution was photolyzed at 300 nm (Rayonet Reactor) and the signal was recorded in mV using a Ca^{+2} electrode. $CaCl_2$ was used to calibrate the electrode; the slope of the calibration curve (22.5) was determined from a plot of log [conc.] *vs*. electrode signal in mV.

The Co^{+2}-cryptate was also investigated. Surprisingly, its photochemistry also followed precedent and released Co^{+2} with nearly the same efficiency, showing little or no effect due to the presence of the paramagnetic Co^{+2}. This is an important finding and opens the way for future studies with ions such as Hg^{+2} that are known paramagnetic triplet quenchers in photochemistry.

Apparently, the o-nitrobenzyl group reacts through the singlet excited manifold which is unaffected by the presence of paramagnets.

References

1. (a) Sellergren, B. *Makromol. Chem*. **1989**, *190*, 2703-2711. (b) Kempe M.; Mosbach, K. *Anal. Lett*. **1991**, *24*, 1137-1145

2. O'Shannessy, D. J.; Ekberg, B.; Mosbach, K. *Anal. Biochem*. **1989**, *177*, 144-151.

3. Steinke, J.; Sherrington, D. C.; Dunkin, I. R. *Advances in Polymer Sciences: Synthesis and Photosynthesis* **1995**, *123*, 81-125.

4. Piletsky, S. A.; Piletska, E. V.; Karim, K.; Freebairn, K. W.; Legge, C. H.; Turner, A. P. F. *Macromolecules* **2002**, *35*, 7499-7504.

5. Sellergren B.; Shea, K. J. *J. Chromatogr.* **1993**, *635*, 31-49.

6. Svenson, J.; Nicholls, I. A. *Anal. Chim. Acta* **2001**, *435*, 19-24.

7. Busch, D.H., Givens, R.S., U.S.Department of Energy Grant Number DE-FG07-96iER14708, Progress Report No. 4 **(**An Interim Report in the Format of a final Report to Inform environmental Management Cleanup Project Managers), "Managing Tight Binding Receptors for New Separations Technologies," Chemistry Department, University of Kansas, Lawrence, KS, for June 15, 2000**.**

8. Givens, R. S.; Lee, J.-I *J. Photoscience* **2003**, *10*, 37 - 48.

9. Givens, R. S.; Conrad, P. G. II; Yousef, A. L.; Lee, J.-I, *Photoremovable Protecting Groups* in "CRC Handbook of Organic Photochemistry and Photobiology," 2nd Edition. W. M. Horspool, ed., in press.

10. Warmuth, R.; Grell, E.; Lehn, J. M.; Bats, J. W.; Quinkert, G. *Helv. Chim. Acta* 1991, *74*, 671.